Digest Journal of Nanomaterials and Biostructures Vol. 7, No. 4, October-December 2012, p. 1509-1518

NANOSTRUCTURAL PROPERTIES OF POLYSTYRENE/La_2O_3 AS A GATE DIELECTRIC OF MOSFET

MANDANA ROODBARI SHAHMIRI, REZA GHOLIPUR[a], ALI BAHARI, NORLDIN MIRNIA
Department of Physics, University of Mazandaran, Babolsar, Iran
[a]Department of Physics, University of Mazandaran, Babolsar, Iran

Scaling of silicon dioxide dielectrics has once been viewed as an effective approach to enhance transistor performance in Complementary Metal-Oxide-Semiconductor (CMOS) technologies. Some issues such as tunneling, leakage currents and light atom penetration through the film are threatening the ultra thin SiO_2 be as a good dielectric for industrial and electron device. We have thus synthesized Ps/La_2O_3 hybrid nano composite with 0/07, 0/14 and 0.28 gr Ps at 80, 300 and 500^{0}C calcinated temperatures for SiO_2 replacing. The Ps/La_2O_3 hybrid nano composites were prepared by a sol-gel method. Nanostructural properties were characterized by using, Energy Dispersive Spectrometers (EDS), X-Ray Diffraction (XRD), Atomic Force Microscopy (AFM), Scanning Electron Microscopy (SEM) and GPS 132A techniques. We measured the dielectric constant (k), capacity (C), quality factor (Q_F) and resistor (R) of Ps/La_2O_3 hybrid nano composite with using GPS 132A technique at a frequency of 120 KHz. The higher dielectric constant (82.67) is found at 300^{0}C with 0.28 gr Ps. Also the square wave voltammetrics peaks current of Ps/La_2O_3 hybrid shows less linearly behavior than that other hybrid nano composites such as anthracene (An)/La_2O_3 hybrid with 0.05 micro molarities of Ps concentration. The obtained results indicate that 0.28 gr Ps/La_2O_3 hybrid nano composite synthesized at 300^{0}C can be used as a good gate dielectric of the next OTFT devices.

(Received June 20, 2012; Accepted September 29, 2012)

Keywords: Nanostructures, Ps/La_2O_3 hybrid nano composite, Sol-Gel method and gate dielectric

1. Introduction

As the dimensions of the microelectronic devices are scaled down, the Complementary Metal-Oxide-Semiconductor (CMOS) technology has pushed the thickness reduction of SiO_2 gate dielectrics. Today, the electronics industry is producing CMOS with very small dimensions [1-10]. For SiO_2 thin film below 2 nm, high leakage current rises to 1-10 A/cm^2 which are unacceptable for stable device performance [11]. Improving the dielectric properties of CMOS structure, it is very important to increase the capacitance of the insulating layer and reduce the leakage current [12]. Many high-k dielectrics have been investigated to replace SiO_2 as possible gate dielectrics, such as Ta_2O_5, ZrO_2, HfO_2, and lanthanide oxide [13-16].

Lanthanide oxide crystallization process at relatively low temperatures (500-600^{0}C) can cause a large leakage current flowing along the grain boundaries [17-19]. Thus to suppress the crystallization at low temperature, Ps atom is doped to La_2O_3 sol. In the present work, Ps/La_2O_3 hybrid nano composites were synthesized with sol- gel method [20-27]. Their nanostructural and electrical properties were studied with using XRD (X-Ray Diffraction), SEM (Scanning Electron Microscopy), X- Powder, CV (Cyclic Voltammeric) and GPS 132A techniques.

* Corresponding author: gholipur_reza@yahoo.com

In this study, we also used voltammetric and electrochemical impedance spectroscopic techniques at PH 6.0 to demonstrate the electrochemical behavior of Organic Composite (OC) on the graphite, Ps/La_2O_3 nano composite modified ethynylferrocene carbon paste electrode.

The results show that the proposed method is highly selective and sensitive in the determination of OC and the quantumic source- channel and/or channel- drain contacts out performing any method reported in the literature on contact sensors [28-30]. We measured the dielectric constant (k), capacity (C), quality factor (Q_F) and resistor (R) of Ps/La_2O_3 nano composite with using GPS 132A technique at a frequency of 120 KHz. The higher dielectric constant (82.67) is found at 300^0C with 0.28 gr Ps. Also the square wave voltammetrics peaks current of Ps/La_2O_3 hybrid shows less linearly behavior than that other hybrid nano composites such as An/La_2O_3 hybrid. The obtained results show that a 0.28 gr Ps/La_2O_3 hybrid nano composite synthesized at 300^0C can be used as a good dielectric of the next OTFT devices.

2. Experimental details

Lanthanum nitrate hexahydrate [$La(NO_3)_3.6H_2O$] was used as the metallic precursors. Acetic acid [CH_3CO_2H] and ethylene glycol monomethyl ether [$CH_3OCH_2CH_2OH$] were used as solvents. Firstly, lanthania solutions were prepared from mixing of lanthanum nitrate hexahydrate with acetic acid with ethylene glycol monomethyl ether separately. Lanthania solutions were stirred vigorously at 50^0C for 1 h. Then solutions with different portions of Ps extracted from polystyrene chloride with the same procedure were mixed and the resultant sol was continuously stirred for 24 hours and kept at room temperature until it turned into a yellowish sol. The 0/07, 0/14 and 0.28 gr Ps were added to the lantana sols. Finally, the stabilized sol was rapidly heated to 60^0C for 10 h. Viscosity and color changed as the sol turned into a stick gel. The gel was heat-treated at 80^0C for 24 h and a fluffy, polymeric precursor was gained. The prepared nanocrystallites calcined at different temperatures at 1 atmosphere pressure. Elemental qualitative analysis was performed with Energy Dispersive Spectrometers (EDS) spectrum. The crystal phases of the nanocrystallites were identified by XRD analysis. Microscopy analysis was performed using SEM technique. Surface morphology was observed by AFM. The dielectric constant and quality factor are measured with using GPS 132A technique.

3. results and discussion

Fig. 1 shows EDS analysis obtained from nanocrystallites confirm that the nanocrystallites consisted of La, Ps and O.

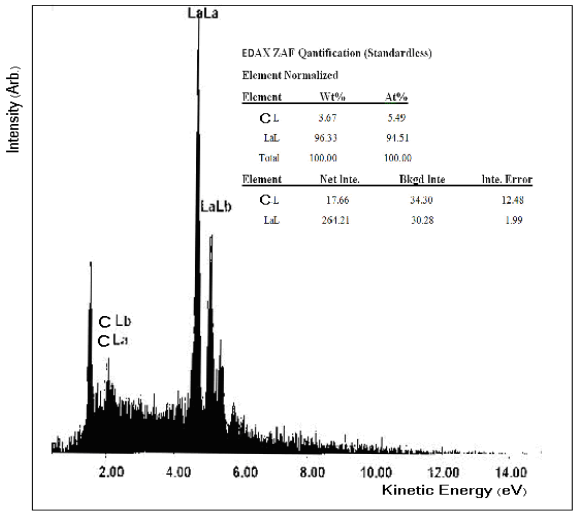

Fig. 1. EDS result for powder sample with x = 5%.

Figure 2 represents the XRD spectra of Ps/La_2O_3sample at different temperatures. As the calcinated temperature of Ps/La_2O_3 nano crystallites increases from 300^0 to 500^0C, peaks with

higher intensities are shifted to higher 2θ. In contrast to amorphous structure at 300^0C, nano crystallites are nearly formed at 500^0C. The size of nano crystallites is become bigger at higher temperatures. As shown in figures 4 through 7, there are different sizes of nano crystallites which can be due to lattice strains in composites. The lattice strain increases with increasing the calcinated temperature and Ps portion for La_2O_3 and Ps crystalline phases. Lattice strain of nano crystallites is determined from the dependence of Full Width-at-Half-Maximum (FWHM) of diffraction lines observed in 2θ range of 25.5^0- 27^0 on $\sin\theta$, according to the Williamson-Hall's [13],

$$\beta\cos\theta = \frac{k\lambda}{L} + 4\sin\theta$$

where β is the width of the diffraction peak at which the intensity has fallen to half the maximum intensity, shape factor k is 0.9 and λ is 1.54 Å.

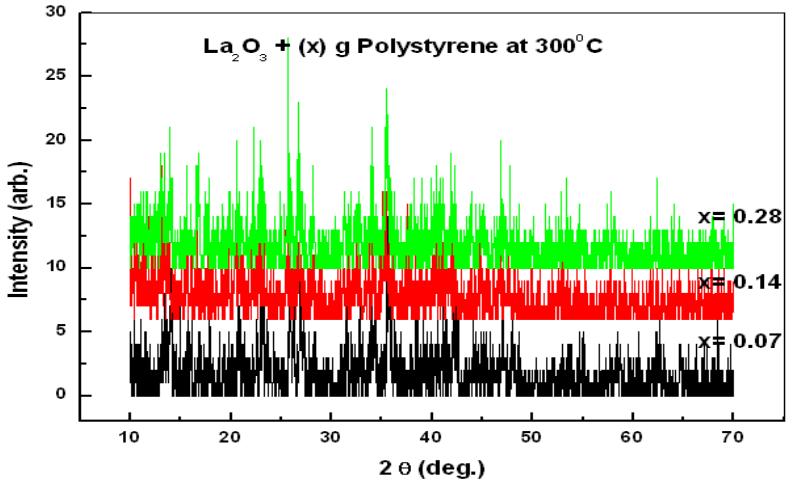

Fig. 2. XRD patterns of Ps/La_2O_3 hybrid composites at different Ps contents.

The pattern of the nano composite film has 3 characteristic peaks at 2θ of 26^0, 35^0 and 46^0 analogous to the characteristic peaks of 0.28 gr Ps/La_2O_3 (figure 3). In addition to the dispersion peak of the amorphous Ps, there is no significant alteration between the Ps nano particles and La_2O_3 nano composite references. It indicates that the degree of crystalinity remains largely invariant. Comparing the intensities and the peak-widths of XRD patterns with different Ps content, it is evident that the Ps/La_2O_3 nano crystallites become more amorphous at 300^0C with 0.28 gr Ps nano particles.

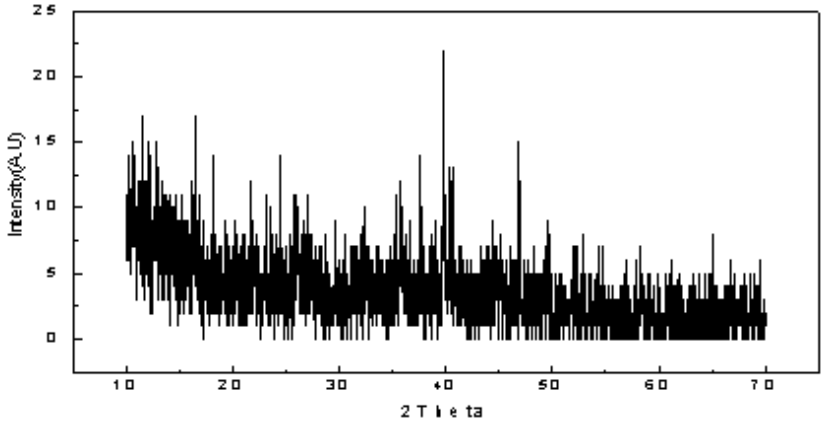

Fig. 3. XRD pattern of 0.28 gr Ps/La_2O_3 composite synthesised at 500^0C with sol- gel method.

As the Ps content in the Ps/La_2O_3 hybrid nano composite increased, nano crystallites were relatively formed in different polycrystalline phases, diffraction peaks shifted slightly to higher 2θ and size nano crystallites increased, as measured with X- Powder method (figures 5 through 7). The size of

nano crystallite of 0.07 gr, 0.14 gr and 0.28 gr Ps/ La_2O_3 hybrid composites at $2\theta = 26.7^0$ is determined with Scherrer equation and X- Powder technique. The grain size values were calculated from Scherrer equation:

$$d = \frac{0.9\lambda}{2\beta \mathrm{Cos}\theta}$$

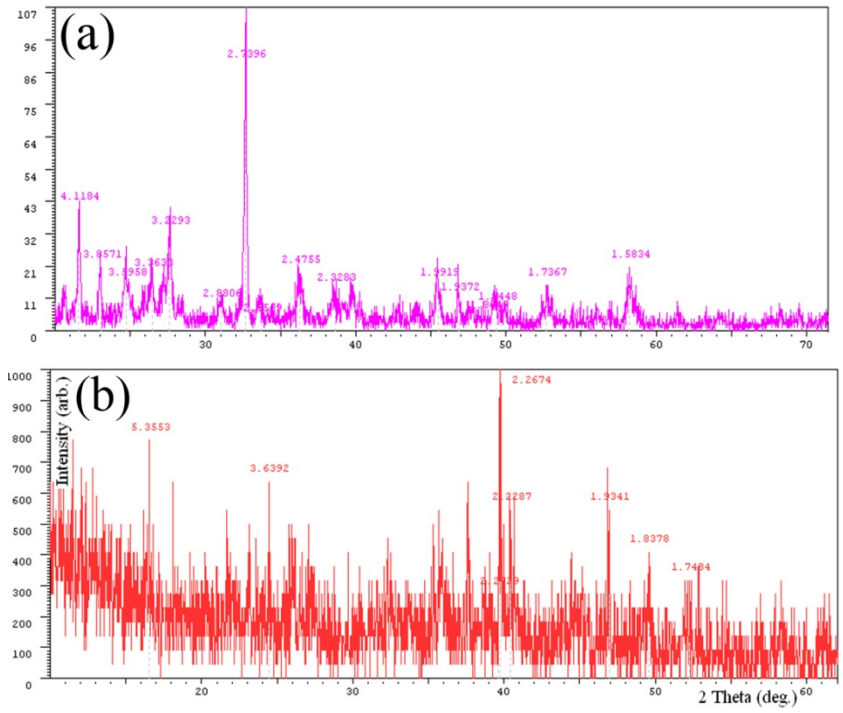

Fig. 4. The size of nano crystallie of 0.28 gr Ps/La_2O_3 hybrid composite phases; (a) at 500^0C and (b) at 300^0C, measured with X- Powder technique

where λ= 0.154 nm, β and θ are the width of the diffraction peak and reflection angle, respectively. The bigger crystallite could be formed at 0.28 g Ps/La_2O_3 hybrid composites at 300^0C. The different size value of crystallite which measured with Scherer equation and X-Powder technique is due to non spherical form of particles (Scherrer equation can give accurate value for spherical particles).

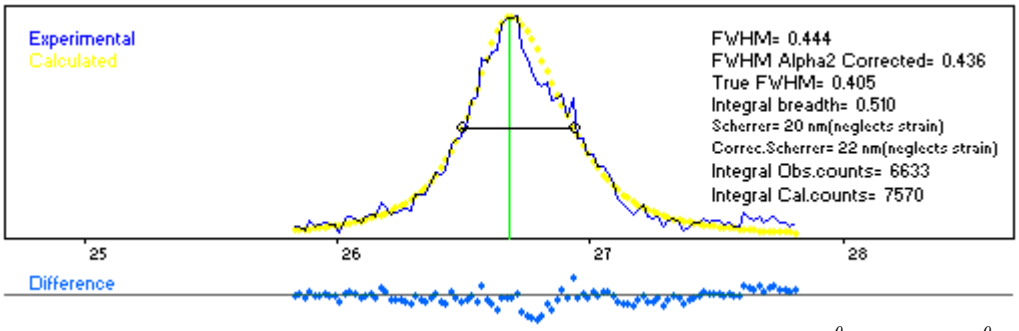

Fig. 5. The size of nano crystallie of 0.07gr Ps/La_2O_3 hybrid composites at $2\theta = 26.7^0$ and $T = 300^0$C, is determined with Scherrer equation (20 nm) and X- Powder technique (22 nm).

The spectra show that the hybrid composite structure has more amorphous structure with 0.28 gr Ps. The amorphous structures obtained at 300^0C calcinated temperature turned crystalline after calcinations at 500^0C (figure 4). Thus the phase obtained was unstable/stable intermediate

phases. From X- powder measurements, we see that crystal size for the three samples varied considerably by changing the proportion of organic (Ps) agents.

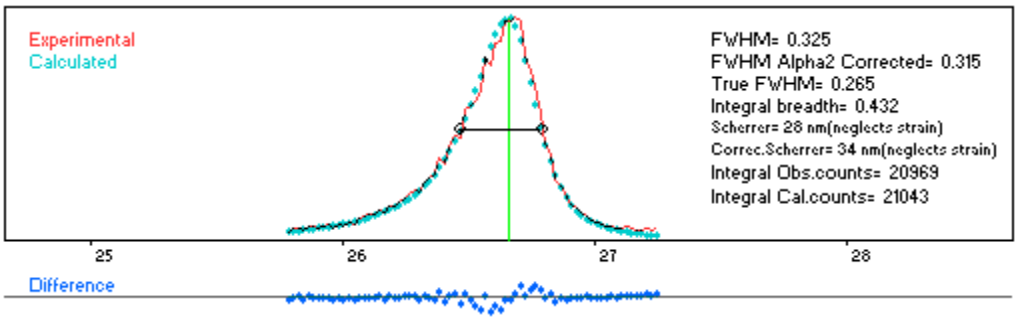

Fig.6. The size of nano crystallite of 0.14 gr Ps/ La_2O_3 hybrid composites at $2\theta = 26.7^0$ and $T = 300^0C$, is determined with Scherrer equation (28 nm) and X- Powder technique (34 nm).

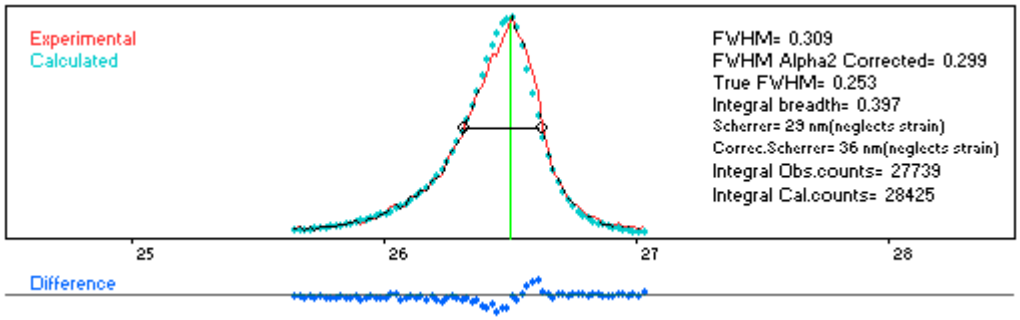

Fig. 7. The size of nano crystallite of 0.28 gr Ps/La_2O_3 hybrid composites at $2\theta = 26.7^0$ and $T = 300^0C$, is determined with Scherrer equation (29 nm) and X- Powder technique (36 nm).

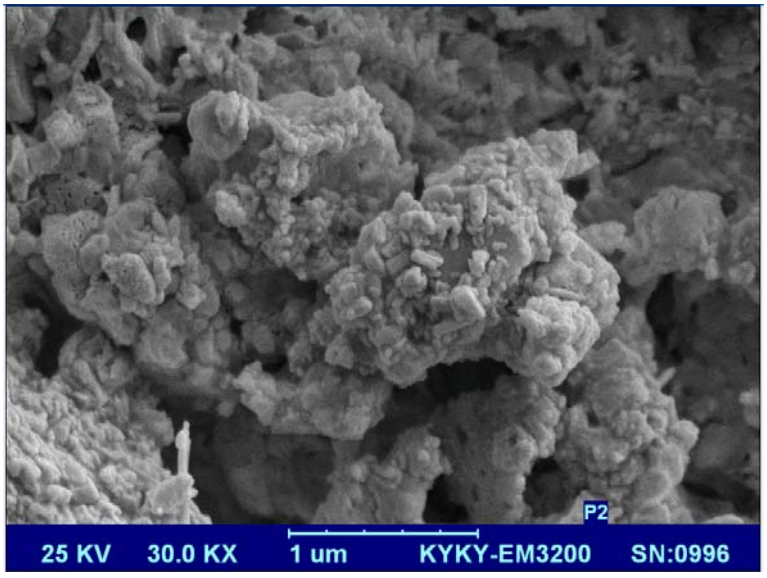

Fig. 8. SEM image of 0.28 gr Ps/La_2O_3 hybrid composites at 80^0C.

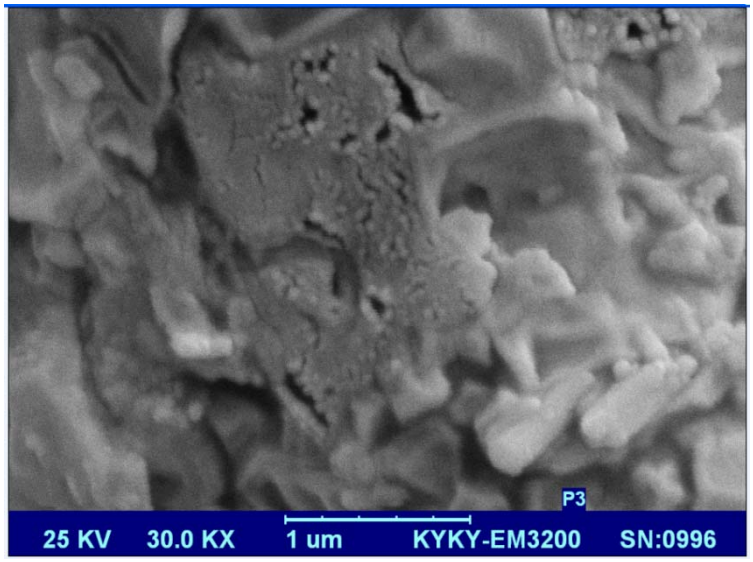

Fig. 9. SEM image of 0.28 gr Ps/La_2O_3 hybrid composites at 300^0C.

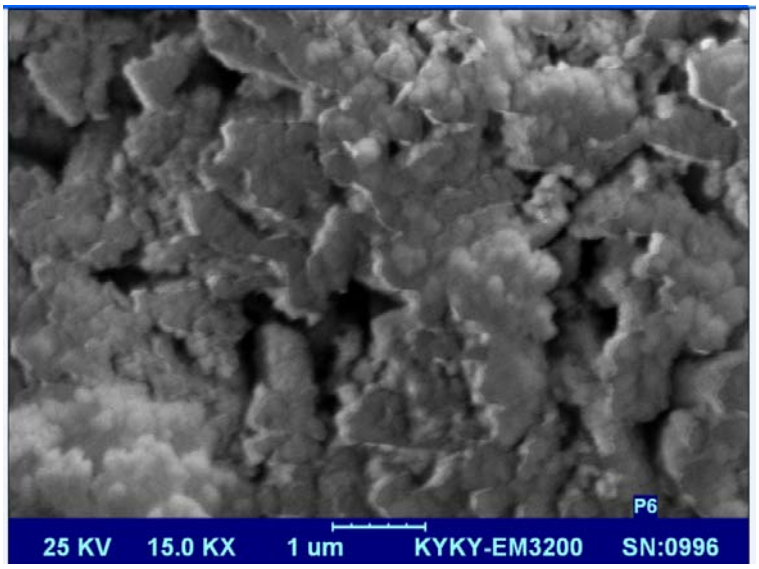

Fig.10. SEM image of 0.28 gr Ps/La_2O_3 hybrid composites at 500^0C.

The morphologies and the surface topography image of untreated Ps/La_2O_3 nanoparticles and Ps/La_2O_3 hybrid nano composites were investigated using SEM technique (see figures 8 through 11). As shown in figure 8, Ps nanoparticles dispersed badly in 0.28 gr PS/ La_2O_3 hybrid nano composites at 80^0C, formed large aggregates. Furthermore, it can also be found that the hybrid nano composites are uniformly dispersed without aggregation with 0.28 gr Ps at 300^0C (figure 9).

Compared with the other Ps portions 0.14 gr Ps at 300^0C (figure 11) and calcinated temperatures with 0.28 gr Ps; 80^0C (figure 8) and 500^0C (figure 10), it is clear that 0.28 gr PS/La_2O_3 hybrid nano composites (figure 9) shows bigger size and very smooth edges. The SEM images show that the morphologies and grains of Ps were not similar due to reduction of carrier mobility (see X- Powder measurements results). Since the Ps has a smaller grain size, it can lead to the roughness peak and a larger roughness valley effect. All the Ps/ La_2O_3 are characterized by a quite smoothly crack– free and homogenous surface. It obviously shows that packing efficiency of

the composite, and dielectric constant increases, meaning the slight agglomeration of the particles especially the smaller – sized one is probably resulted from the high temperature curing process. The results demonstrated that proportion of the Ps nano particles in La_2O_3 contents influenced crystal size and morphology.

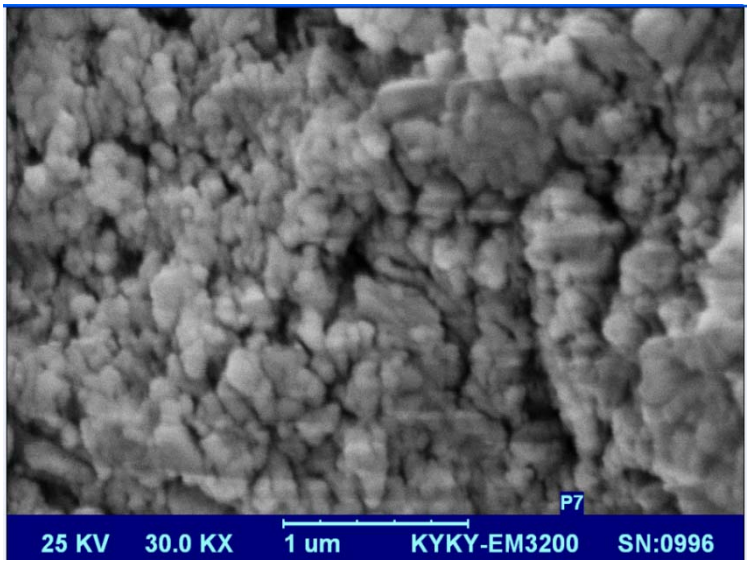

Fig.11. SEM image of 0.14 gr Ps/La_2O_3 hybrid composites at 300^{0}C.

Furthermore, the smoother topography of Ps surface results in less distortion of the crystalline structure of 0.28 gr Ps/ La_2O_3 (figure 9) compared with other Ps portion of Ps in Ps/La_2O_3 and calcinated temperature, we expect there should be less carrier scattering at the roughness peaks and the roughness valley effect. It is confirmed by looking at figure 9 which exhibits more compact structure and comparing the dielectric constant of hybrid nano composite in table 1 in that the maximum dielectric constant is 82.67 for Ps/ La_2O_3 hybrid nano composite synthesized at 300^{0}C with 0.28 gr Ps content. This structure with the fewer amounts of voids can increase the dielectric constant of the Ps/ La_2O_3 hybrid nano composite at 300^{0}C with 0.28 gr Ps content due to more packed composite and filled voids between large particles with small Ps particles.

In parallel to above studies, nano crystallites in the SEM images (figures 8-11), showed similar surface roughness which can affect the electrical properties of the Ps/La_2O_3 nano crystallites. Moreover, island-shaped morphology on the Ps/ La_2O_3 hybrid nano composites calcined at 300^{0}C in 0.28 gr Ps/ La_2O_3 exhibits the homogeneous and uniform surface structure. We see that this hybrid nano composite has tight surface and thus good blocking function to prevent the leakage and tunneling currents as well as reduce the trap density.

Figs 12 (a, b) show AFM topographical images of synthesized Ps/La_2O_3 nanocrystallites at room temperature and at 700^{0}C, respectively. The scan size was 4.031 pm^2. S_a of the synthesized Ps/La_2O_3 nanocrystallites is about 88.152 nm. Uniform surface was observed. Calcined nanocrystallites at 700^{0}C, showed rougher surface with many grains, as well as crystallites contours are clearly visible. Ps/La_2O_3 nanocrystallites had partly a flat and smooth surface morphology. In addition, Fig. 12c shows the images of height distribution of polystyrene/La_2O_3 calcined nanocrystallites at 700^{0}C. These images obviously revealed that, heights distribution at synthesized polystyrene/La_2O_3 nanocrystallites is more than that had been mentioned before.

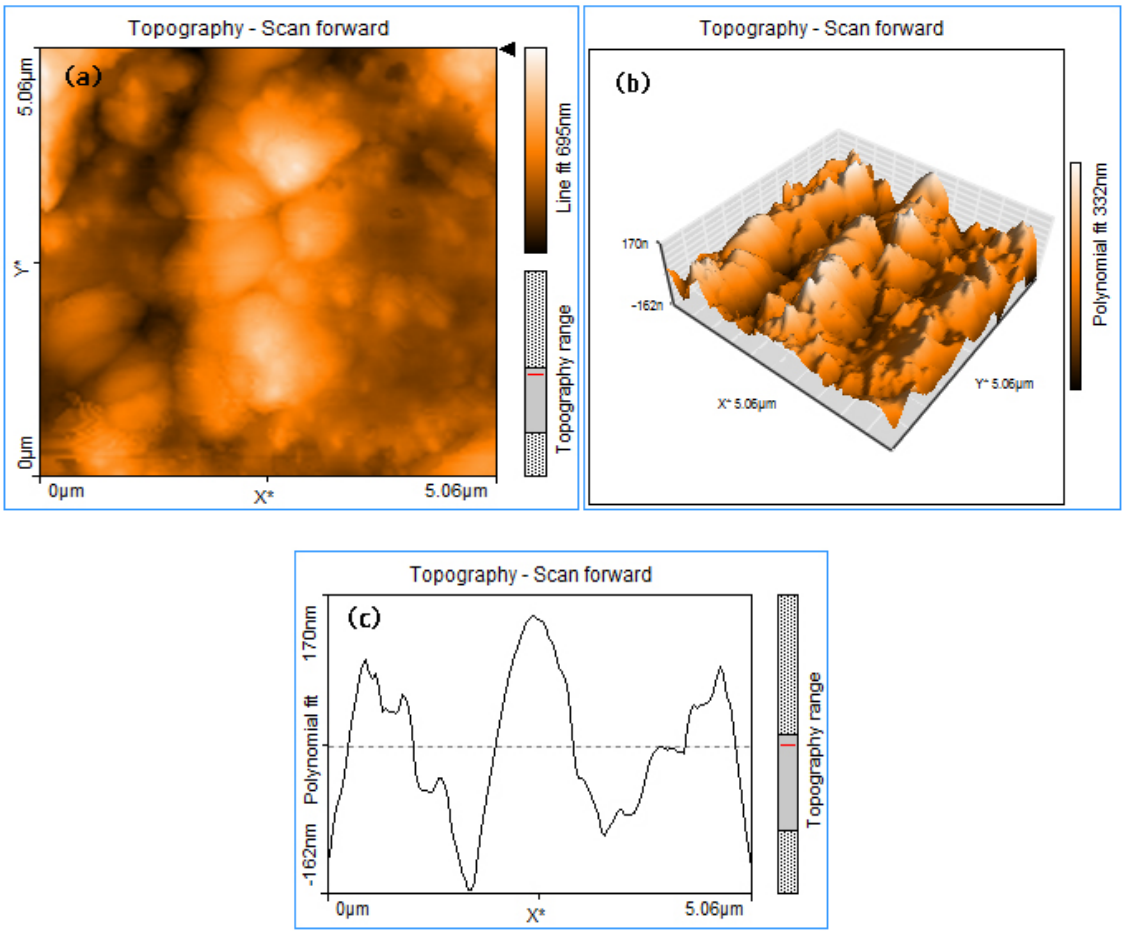

Fig. 12. (a, b) AFM topography images of polystyrene/La_2O_3 at 700^{0}C (c) the images of height distributions of polystyrene/La_2O_3 nanocrystallites.

Table 1. The dielectric constant (k), capacity (C), quality factor (Q_F), the loss-rate of energy of capacitor (D_F) and resistor (R) of Ps/ La_2O_3 nano composite with using GPS 132 A technique at a frequency of 120 KHz. The higher dielectric constant (82.67) is found at 300^{0}C with 0.28 gr Ps.

R (KΩ)	C (nF)	Q_F (=1/ D_F)	k	T (^{0}C)	… gr Ps
35.9	0.023	1.56	30.3	80	0.14
91.6	0.046	1.91	46.2	80	0.28
47.8	0.081	0.98	67.8	300	0.07
88.2	0.016	1.88	34.6	300	0.14
75.4	0.066	2.81	82.67	300	0.28
85.4	0.021	1.33	24.7	500	0.14
105.1	0.027	2.05	57.72	500	0.28

As temperature increases to 500^{0}C, Ps/La_2O_3 nano crystallites phases as well as k value have been appeared due to amplification dipole moments. It is clear that from 80^{0}C to 500^{0}C, the maximum value of k is obtained at 300^{0}C calcinated temperature with 0.28 gr Ps and Q_F value increases. Higher Q_F value indicates a lower rate of energy loss respect to the stored energy of the capacitor as demonstrated in,

$$Q_F = 2\pi \times \frac{\text{Energy Stored}}{\text{Energy dissipated per cycle}}$$

D_F value defined with give the loss-rate of energy of capacitor and varies with the dielectric material and decreased at higher temperature as presented in table 1,

$$D_F = 1/Q_F$$

4. Conclusion

In the present work, the structural and electrical properties of the Ps/La_2O_3 nano crystallites prepared by sol-gel method were studied. XRD analysis revealed that as the Ps content in the nano crystallites increases from 0.07 gr to 0.28 gr Ps, peaks intensity decreased and broadened. From the XRD pattens, it is clear that the sample has amorphous structure which can reduce the leakage and tunneling currents. Poole–Frenkel effect has been observed due to the trap levels originated from defect levels, indicate that adsorbed oxygen, polystyrene or lanthanum atoms present in the grain boundary regions can change the nano structural (electrical and nano structural properties). Since the permittivity value of Ps/La_2O_3 is higher for 0.28 gr Ps content (82.67) than that for the other Ps portions and calcinated temperatures, we can suggest 0.28 gr Ps/La_2O_3 dielectric synthesized at 300^0C, can be introduced as a good gate dielectric material for the next OTFTs generations. The reasons are reduction of leakage current density, tunneling current and preventing boron diffusion through the thin gate dielectric (Ps/La_2O_3 hybrid composites) structures. The obtained results also indicate that proportion of the organic materials in La_2O_3 contents can influence crystal size and morphology of hybrid samples.

References

[1] A. Bahari, U. Robenhagen, P. Morgen, Z.S. Li, Phys. Rev B **72,** 205323 (2005).
[2] A. Bahari and R. Gholipur, J. Mater. Sci.: Materials in Electronics, in publish (2012).
[3] O. Carp, C. L. Huisman, A. Reller, Prog. Solid State Chem **32,** 177 (2004).
[4] A. Bahari, P. Morgen, K. Pedersen, Z.S. Li, J. Vac. Technol B **24,** 2119 (2006).
[5] L. Dell, S. Savin, A. Chadwick and M. Smit, J. Phys. Chem. C **111,** 13740 (2007).
[6] A. Bahari, M. Roodbari Shahmiri and N. Mirnia, IJTP, DOI: 10.1007/s10773-012-1231-6 (2012).
[7] L. Dell, S. Savin, A. Chadwick and M. Smit, Faraday Discuss **134,** 83 (2007).
[8] J. J. Chambers and G. N. Parsons, Appl. Phys. Lett **77,** 2385 (2000).
[9] M. Roodbari, M. Rezaee and N. Shahtahmasbi, Int. J. ChemTech. Research **3,** 1681 (2011).
[10] A. Bahari, JNS **1,** 54(2012).
[11] C. Zhao, T. Witters, B. Brijs, H. Bender, O. Richard, M. Caymax, T. Heeg, J. Schubert, V. Afanas'ev, A. Stesmans, D.G. Schlom, Appl. Phys. Lett **86,** (2005) 132903.
[12] H. F. Luan, B. Z. Wu, L. G. Kang, B.Y. Kim, R. Vrtis, D. Robert and D. L. Kwong, IEDM'98 Technical Digest, San Francisco **567,** 609(1998).
[13] M. Riazian and A. Bahari, PRAMANA **78**(2), 319 (2012).
[14] X. Yu, C. Zhu, M. F. Li, A. Chin, A. Y. W. T. Du, Wang, D. L. Kwong, Appl. Phys. Lett **85,** 2893(2004).
[15] H. Guoa, X. Yangb, T. Xiaob, W. Zhanga, L. Loub and J. Mugnierc, App. Surf. Sci **230,** 215(2004).
[16] G. H. Chen, Z. F. Hou, X. G. Gong, Comput. Mater. Sci **44,** 46(2008).
[17] M. Zaharescu, V. S. Teodorescu, M. Gartner, M. G. Blanchin, A. Barau, M. Anastasescu, J. Non-Crystalline Solids **354,** 409 (2008).
[18] A. Bahari, Z. Khorshidi, A. Ebrahimi and A. Rezaeian, Innova Ciencia **4**(4), 62 (2012).
[19] U. Ehrke, A. Sears, L. Alff, D. Reisinger, Appl. Surf. Sci **231,** 598 (2004).
[20] A. Balamurugan, S. Kannan, S. Rajeswari, Materials Lett **57,** 4202 (2003).
[21] P. Y. Kuei, J. D. Chou, C. T. Huang, H. H. Ko, S. C. Su, J. Crystal Growth **314,** 8(2011).
[22] S. H. Jeonga, I. S. Baea, Y. S. Shina, S. B. Leea, H. T. Kwakb, J. H. Booa, Thin Solid Films **475,** 354 (2005).
[23] G. D. Wilk, R. M. Wallace, J. M. Anthony, J. Appl. Phys **89,** 5243 (2001).

[24] A. Bahari and A. Ramzannejad, Int. J. Modern Phys B **26,** 1250080 (2012).
[25] A. Bahari, Z. Khorshidi , R. Gholipour, T. Taghipoor and A. Rezaeian, Am. J. Sci. Research **54, 19** (2012).
[26] N. Gang, Y. Wu, B. Lili, G. Hao, Z. Wenhao and G. Jinzhang, **51,** 1644 (2006).
[27] B. Jaleh, M. Shayegani Madad, M. Farshchi Tabrizi, S. Habibi, R. Golbedaghi and M.R. Keymanesh, J. Iran. Chem. Soc **8,** S161 (2011).
[28] A. Ensafi, M. Taei, T. Khayamian, H. Karimi-Maleh, F. Hasanpour, J. Solid State Electrochem **14,** 1415 (2010).
[29] W. Y. Su, S. H. Cheng, Electroanalysis **22,** 707 (2010).
[30] A. A. Ensafi, H. Karimi-Maleh, S. Mallakpour, M. Hatami, Sens. Actuators B **155,** 464 (2011).